New Phytologist

Research

Genetic and transcriptomic analysis of the *Bradyrhizobium* T3SS-triggered nodulation in the legume *Aeschynomene evenia*

Alicia Camuel[1,2], Djamel Gully[1,2], Marjorie Pervent[1,2], Albin Teulet[1,3], Nico Nouwen[1,2], Jean-François Arrighi[1,2]* and Eric Giraud[1,2]*

[1]IRD, Laboratoire des Symbioses Tropicales et Méditerranéennes (LSTM), UMR IRD/Institut Agro Montpellier/INRAE/Université de Montpellier/CIRAD, TA-A82/J- Campus de Baillarguet, 34398, Montpellier Cedex 5, France; [2]PHIM Plant Health Institute of Montpellier, Université de Montpellier, IRD, CIRAD, INRAE, Institut Agro, 34398, Montpellier Cedex 5, France; [3]University of Cambridge, Sainsbury Laboratory (SLCU), Cambridge, CB2 1LR, UK

Authors for correspondence:
Eric Giraud
Email: eric.giraud@ird.fr

Jean-François Arrighi
Email: jean-francois.arrighi@ird.fr

Received: *21 May 2024*
Accepted: *2 September 2024*

New Phytologist (2024)
doi: 10.1111/nph.20139

Key words: *Aeschynomene evenia*, effectors, legume, Nod factor independent, rhizobium, signalling pathway, symbiosis.

Summary

- Some *Bradyrhizobium* strains nodulate certain *Aeschynomene* species independently of Nod factors, but thanks to their type III secretion system (T3SS). While different T3 effectors triggering nodulation (ErnA and Sup3) have been identified, the plant signalling pathways they activate remain unknown.
- Here, we explored the intraspecies variability in T3SS-triggered nodulation within *Aeschynomene evenia* and investigated transcriptomic responses that occur during this symbiosis. Furthermore, *Bradyrhizobium* strains having different effector sets were tested on *A. evenia* mutants altered in various symbiotic signalling genes.
- We identified the *A. evenia* accession N21/PI 225551 as appropriate for deciphering the T3SS-dependent process. Comparative transcriptomic analysis of *A. evenia* N21 roots inoculated with ORS3257 strain and its Δ*ernA* mutant revealed genes differentially expressed, including some involved in plant defences and auxin signalling. In the other *A. evenia* accession N76, all tested strains nodulated the *AeCRK* mutant but not the *AeNIN* and *AeNSP2* mutants, indicating a differential requirement of these genes for T3SS-dependent nodulation. Furthermore, the effects of *AePOLLUX*, *AeCCaMK* and *AeCYCLOPS* mutations differed between the strains. Notably, ORS86 nodulated these three mutant lines and required for this both ErnA and Sup3.
- Taken together, these results shed light on how the T3SS-dependent nodulation process is achieved in legumes.

Introduction

In rhizobium/legume symbiosis, the interaction leads to the formation of a symbiotic organ, the nodule, in which the bacteria fix dinitrogen for the plant's benefit. This interaction generally involves an exchange of diffusible signals between the two partners, in which the rhizobial Nod factors (NFs) are recognized as the key signal that governs the nodule formation and its concomitant infection by the bacteria (Perret *et al.*, 2000; Oldroyd, 2013). However, alternative symbiotic processes independent of the NF signal have also been described (Giraud *et al.*, 2007; Okazaki *et al.*, 2013, 2016). For instance, some tropical legumes of the *Aeschynomene* genus, such as *Aeschynomene indica* and *Aeschynomene evenia*, are nodulated by photosynthetic *Bradyrhizobium* strains (ORS278 and BTAi1) that lack the canonical *nodABC* genes necessary for NF synthesis (Giraud *et al.*, 2007). The bacterial determinant(s) that trigger(s) this NF-independent nodulation process still remain unknown. Interestingly, in *in vitro* conditions, *A. indica* can also be nodulated by a large diversity of nonphotosynthetic bradyrhizobia (Okazaki *et al.*, 2016; Camuel *et al.*, 2023). Contrary to the photosynthetic strains, this interaction is possible only if the bacteria have a functional type III secretion system (T3SS). This secretory machinery permits to inject bacterial proteins, named type III effectors (T3Es), directly into the host cell, modulating the host immunity and inducing nodule organogenesis (Teulet *et al.*, 2022). In the case of the T3SS-dependent symbiosis between *B. vignae* ORS3257 strain and *A. indica*, it has been shown that at least five T3Es are required: NopM and NopP repress the plant defence immunity, NopT and NopAB are required for bacterial infection, and finally, ErnA activates nodule organogenesis (Teulet *et al.*, 2019). Interestingly, with other *Bradyrhizobium* strains, *A. indica* nodule organogenesis is activated by different T3Es, such as Sup3 encoding a putative SUMO protease in Nas96.2, ORS86 and WSM1744 strains, and three unknown putative T3Es (named Ubi1, Ubi2 and Ubi3) in the LMTR13 strain (Camuel *et al.*, 2023). These various T3Es, proposed to be called ET-Nods for effectors triggering nodulation

*These authors contributed equally to this work.

(Busset *et al.*, 2021), are very different from each other suggesting variations in the *modus operandi* to activate the T3SS-dependent nodulation programme in *Aeschynomene*.

During the last two decades, significant progress has been made to identify the plant genetic determinants that are involved during the NF-dependent symbiotic process. Using *Medicago truncatula* and *Lotus japonicus* as model plants, the main actors governing symbiosis have been identified (Roy *et al.*, 2020). In brief, upon NFs perception, a pair of LysM-RLK receptors (MtNFP/LjNFR5–MtLYK3/LjNFR1) and the co-receptor SYMRK (MtDMI2) activate nuclear-associated calcium oscillations via several cation channels (CASTOR/MtDMI2 and POLLUX/MtCNGC15) and nucleoporins (LjNUP85, LjNUP133 and NENA). A Ca^{2+}/calmodulin-dependent kinase (CCaMK/MtDMI3) decodes these calcium oscillations and phosphorylates the transcription factor CYCLOPS/IPD3 which, together with other transcription factors (NSP1 and NSP2), activates the expression of NIN, the master regulator of nodule initiation and infection thread development (Feng *et al.*, 2021).

To advance in the understanding of the NF-independent, T3SS-independent symbiosis elicited by photosynthetic bradyrhizobia, *Aeschynoemne evenia* was chosen to develop functional studies (Arrighi *et al.*, 2012). Its small diploid genome size ($2n = 20$, 415 Mb/1C), its selfing nature and its prolific seed production were strong criteria to select this species as model. The *A. evenia* inbred CIAT22838 line (referred here as N76) was used to establish a reference genome sequence and to develop a forward genetic approach. By screening 70 000 ethyl methane sulfonate (EMS)-mutagenized seedlings for defects in nodulation with the photosynthetic *Bradyrhizobium* model strain ORS278, several mutant lines with a complete absence of nodulation were identified and shown to have mutations in key determinants (*AePOLLUX, AeCCaMK, AeCYCLOPS, AeNSP2* and *AeNIN*) of the NF-signalling pathway (Quilbé *et al.*, 2021, 2022). This indicates that the NF/T3SS-independent signalling process recruits several conserved symbiotic determinants acting downstream of the NF receptors. Interestingly, this mutant-based approach also identified a new symbiotic gene *AeCRK* encoding a cysteine-rich receptor kinase (CRK) that plays a key role in the establishment of NF-independent symbiosis with photosynthetic *Bradyrhizobium* strains (Quilbé *et al.*, 2021, 2022).

In contrast to the two above-described symbiotic processes, our knowledge of the NF-independent, T3SS-dependent process elicited by nonphotosynthetic bradyrhizobia remains extremely limited. It is hypothesized that ErnA, which has been shown to target the host cell nucleus and interact with nucleic acids, may act by modulating plant genes expression, while Sup3, also targeted to the host nucleus but containing a C-terminal small ubiquitin-like modifier (SUMO)-Protease domain, may act by deSUMOylation of specific nuclear plant protein targets (Teulet *et al.*, 2019; Camuel *et al.*, 2023). Thus, these two distinct ET-Nods might have different plant targets to trigger nodulation. Furthermore, within *A. evenia*, a high genetic diversity was observed, which in contrast to nodulation with photosynthetic *Bradyrhizobium* strains, has a strong impact on nodulation by *Bradyrhizobium* strains using a NF-independent, T3SS-dependent process (Okazaki *et al.*, 2016; Chaintreuil *et al.*, 2018). This indicates that within *A. evenia*, intraspecific variations of some specific determinant(s) govern the outcome of the symbiotic interaction when the T3SS is involved. Notably, the *A. evenia* N76 accession that is used as model plant to decipher the symbiotic molecular mechanism mediated by photosynthetic bradyrhizobia is not or very badly nodulated by nonphotosynthetic strains using their T3SS (Okazaki *et al.*, 2016).

In this study, to better understand how the NF-independent, T3SS-dependent symbiosis is operated, we have first explored the intraspecies variability in nodulation within *A. evenia* and evidenced that the line N21 is well nodulated by nonphotosynthetic *Bradyrhizobium* strains in a T3SS-dependent fashion. Using *A. evenia* N21, we performed a comparative RNA-seq analysis of roots inoculated with *Bradyrhizobium* ORS3257 and its Δ*ernA* mutant to identify the host plant genes whose expression is impacted by ErnA. Additionally, we exploited the *A. evenia* N76 mutant lines impaired in nodulation with the ORS278 strain, to determine whether some nonphotosynthetic *Bradyrhizobium* strains can bypass, thanks to their T3SS, the requirement of certain symbiotic signalling genes for nodulation.

Materials and Methods

Plant material and growth conditions

All accessions of *Aeschynomene* used in this study are detailed in Supporting Information Table S1. The *A. evenia* (C. Wright) mutant lines affected in the common symbiotic pathway genes were obtained from the phenotypic screen of an EMS-mutagenized population derived from the reference N76 line (Quilbé *et al.*, 2021). Seeds were scarified for 40 min with sulfuric acid (96% v/v) and rinsed with distilled water. Germination was induced overnight at room temperature in distilled water for wild-type (WT) seeds, and with 0.01% (v/v) of ethrel (BAYER) for mutant's seeds. Germinated seeds were transferred onto 0.8% water agar plates and incubated overnight at 34°C. *A. evenia*, and *A. indica* seedlings were cultured in cultivation chamber as previously described (Arrighi *et al.*, 2012).

Bacterial strains and growth conditions

All bacterial strains and derivative mutants used are listed in Table S2. The *Bradyrhizobium* strains were grown in YM or AG medium at 28°C (Vincent, 1970; Sadowsky *et al.*, 1987). *Agrobacterium rhizogenes* Arqua1 strain was grown at 28°C on AG medium. *Escherichia coli* strains were grown at 37°C in modified Lysogeny Broth (LB) medium (Sambrook *et al.*, 1989). When required, the media were supplemented with the appropriate antibiotics at the following concentrations: 20 μg ml^{-1} nalidixic acid, 20 μg ml^{-1} cefotaxime, 50–100 μg ml^{-1} kanamycin and 100–200 μg ml^{-1} spectinomycin.

Sup3 transfer into ORS3257 and ORS3257Δ*ernA* strains

The complete *sup3* (JAAVLW01_10281) gene of WSM1744 was amplified by PCR using the primers (GGCCTAT**ACTAGT**A

CCGAGGGGGACATGAAGTTCCAATCCACCAACTG/CAGCCA**ACTAGT**TTAGCCCAAGCCGGGATGAGCCAGTCGACTC) and the Phusion™ High-Fidelity DNA Polymerase (Thermo Scientific, Waltham, MA, USA). The PCR product was cloned into the SpeI site of the plasmid pVO155-*pm-ernA* (Camuel *et al.*, 2023) in order to put the *sup3* gene under the control of the $ernA_{ORS3257}$ promoter. The construct was transferred into ORS3257 strain by single crossing over as described previously (Teulet *et al.*, 2019).

Symbiotic analysis

For each condition, 8–10 plants were inoculated with a bacterial strain and symbiotic properties were analysed 21 d postinoculation (dpi) as described previously (Bonaldi *et al.*, 2010b). Cytological analysis of the nodules was performed as described (Songwattana *et al.*, 2021). The experiments were carried out at least in duplicate.

RNA-seq analysis

Aeschynomenae evenia N21 plants were inoculated with the ORS3257 WT strain and its Δ*ernA* mutant. At 2, 3, 4 and 9 d after inoculation, the root system of 12 plants per conditions were pooled, immediately frozen in liquid nitrogen and subsequently grounded into a fine powder. For each time point, three replicates were done. For total RNA extraction, 100 mg of the powder was taken and used in the protocol as described by Chomczynski & Sacchi (1987). RNA quality and concentration were evaluated using a NanoDrop 2000/200c (Thermo Fisher) and an Agilent 2100 Bioanalyzer according to the manufacturer's instructions. The cDNA library was constructed as described previously (Gully *et al.*, 2018). cDNA libraries were sequenced on a full S1 flow-cell (NovaSeq) in single read 100 nt mode. Image analysis, base calling and quality filtering were performed by MGX platform (GenomiX, Montpellier, France). The 'raw reads' were filtered to remove low quality and contaminant reads, including adaptor sequences, DNA or PCR duplicates, which generated trimmed reads. The trimmed reads were mapped to the reference genome *Aeschynomene_evenia*_v.1.0 (Quilbé *et al.*, 2021) using the NF-core/rnaseq pipeline (Ewels *et al.*, 2020; Patel *et al.*, 2020). Briefly, reads were aligned to the reference genome using STAR (Dobin *et al.*, 2013) and gene expression was quantified with Salmon (Patro *et al.*, 2017). Differentially expressed genes (DEG) were identified using DESEQ2 (Love *et al.*, 2014) as implemented in the Diane pipeline (Cassan *et al.*, 2021) and defined using a false discovery rate (FDR) of 0.05 and an absolute log_2-transformed fold change (Log_2FC) greater than 1. Table S3 gives for each library a summary of raw Illumina sequencing and filtered reads after trimming and alignment to *A. evenia* N76 genome.

Real-time quantitative PCR

Reverse transcription was performed using 1 µg of RNA per sample using oligo(dT) (Promega) and Reverse Transcriptase SuperScript II (Invitrogen). Real-time qPCR assays were performed using the Takyon Low ROX SYBR MasterMix dTTP Blue (Eurogentec, Liège, Belgium) according to the manufacturer's instructions. Specific primers were designed with LIGHTCYCLER software using the annotated *A. evenia* N76 genome and are listed in Table S4. The three independent biological replicates for each timepoint were analysed. Expression levels were normalized using the *AeEF1-α* and *AeUbi* reference genes as reported previously (Quilbé *et al.*, 2022).

Hairy root transformation with *Agrobacterium rhizogenes*

Plasmid *p35S-ernA* containing *ernA* under the control of the 35S promoter (Teulet *et al.*, 2019), and the empty vector pJCV51 with the DsRed marker (https://gateway.psb.ugent.be), were used for hairy root transformations. *A. evenia* root transformation was performed following previously described procedures (Bonaldi *et al.*, 2010a).

Results

Aeschynomene evenia PI 225551 (N21) is permissive to nodulation by T3SS-containing bradyrhizobia

The model strain *Bradyrhizobium vignae* ORS3257 was previously shown to nodulate in a NF-independent/T3SS-dependent fashion *A. indica* LSTM19 (N19). This species represents a convenient host plant for nodulation tests, but its allopolyploid genome renders plant gene analysis intricated (Arrighi *et al.*, 2012; Chaintreuil *et al.*, 2018). To circumvent these complications, we aimed at identifying an accession in the closely related and diploid *A. evenia* species that equals the nodulation behaviour of *A. indica* N19. In the first approach, we examined a collection of 20 *A. evenia* accessions for their ability to be nodulated by strain *B. vignae* ORS3257. Three distinct groups can be distinguished (Fig. 1a): (1) Group 1 with nine accessions that were not or very rarely nodulated; (2) Group 2 with eight accessions, including N76, that were weakly nodulated with an average of one to seven nodules per plant, and finally; (3) Group 3 with three accessions (N21-also named PI 225551/N57/N108), that were well nodulated with an average of 25–30 nodules per plant, a level of nodulation comparable to the one observed on *A. indica* N19. Interestingly, these three last accessions were found grouped together in a NJ tree previously obtained and constructed from the allelic data of SSRs markers, which indicates their genetic proximity (Chaintreuil *et al.*, 2018). While the geographical origin of one accession (N108) is unknown, the other two (N21 and N57) originate from the same region in West Africa (in the vicinity of the Victoria falls) (Table S1), suggesting that these three accessions may correspond to the same ecotype. As genomic sequence data are available for the N21 accession (Quilbé *et al.*, 2022), we decided to focus on this one.

Since the symbiotic phenotype (nodule number and the pattern of infection) strongly differs between *Bradyrhizobium* strains using the T3SS (Okazaki *et al.*, 2016; Camuel *et al.*, 2023), we compared the nodulation properties of 13 different *Bradyrhizobium* strains on the two *A. evenia* accessions (N76 and N21), as

New Phytologist

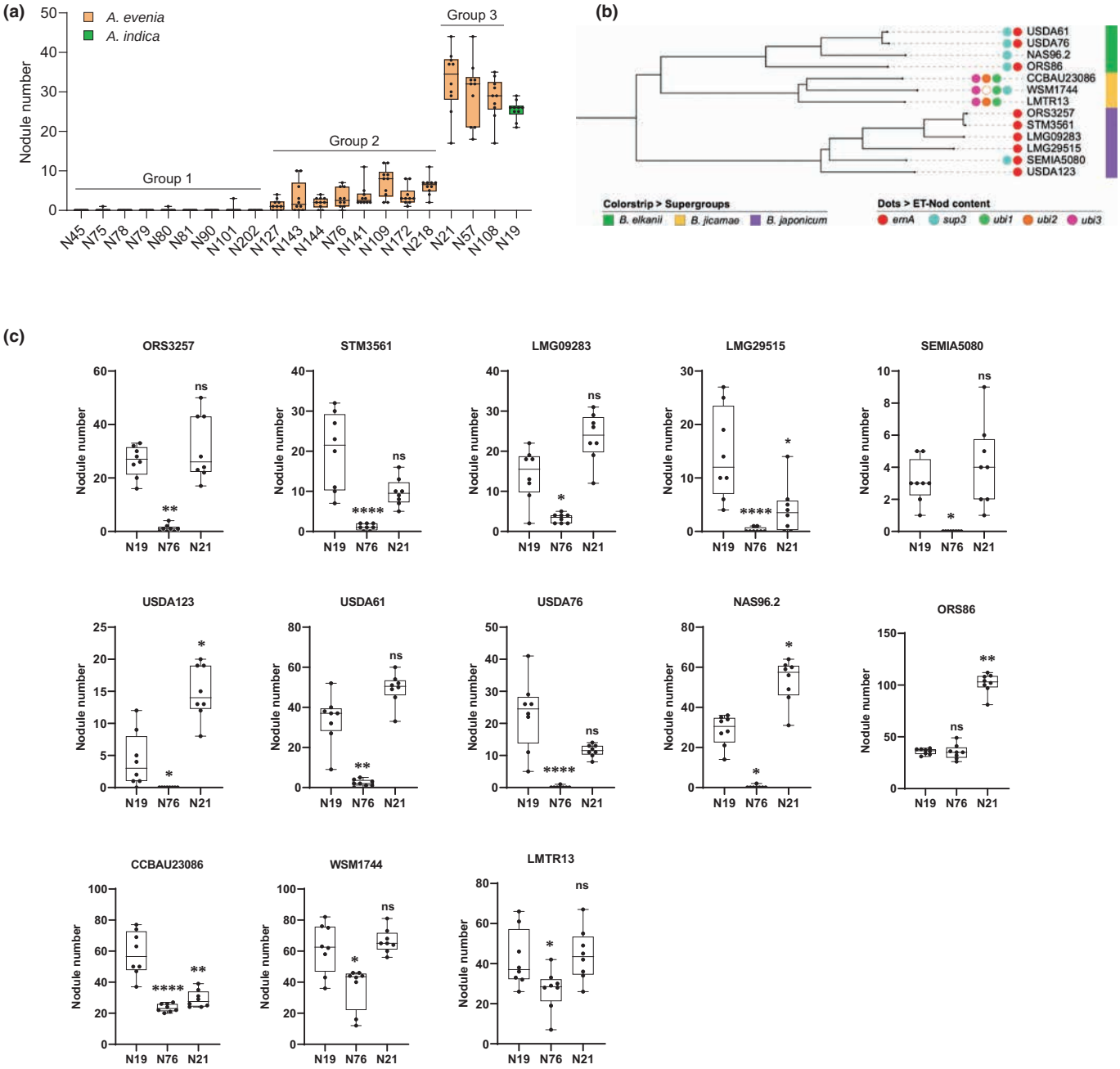

Fig. 1 Identification of *Aeschynomene evenia* ecotype PI 225551 (N21) as an appropriate model for deciphering the type III secretion system (T3SS)-dependent symbiotic process. (a) Nodule number of different accessions of *A. evenia* ssp. *evenia* plants at 21 d postinoculation (dpi) with the model strain ORS3257. Box plots show the results of one of the two experiments performed independently on 10 plants for each accession. The green colour refers to *Aeschynomene indica* N19 while the orange colour refers to *A. evenia* ssp. *evenia* accessions. (b) Phylogenomic tree of the 13 *Bradyrhizobium* strains used in this study obtained with the pruning tree option in iTOL (https://itol.embl.de/) (Letunic & Bork, 2021), from a previously phylogenomic analysis (Camuel *et al*., 2023). Strains from three phylogenomic supergroups were used in our analysis: *Bradyrhizobium japonicum* (six strains), *Bradyrhizobium elkanii* (four strains) and *Bradyrhizobium jicamae* (three strains). The putative ET-Nods content for each strain is indicated by coloured dots referenced in the key. (c) Nodule number induced by each strain on three different *Aeschynomene* accession plants (N19, N76 and N21) at 21 dpi. Box plots show the results of one of the two experiments performed independently on eight plants for each accession. ****, $P < 0.0001$; **, $P < 0.01$; *, $P < 0.05$, significant differences between the *A. indica* (N19) ecotype and the two others *A. evenia* accessions (N76 and N21) using a nonparametric Kruskal–Wallis test, ns, not significant. It is to note that the 'pseudo-nodules' induced by LMTR13 on *A. evenia* N76 are extremely small and as a result the exact nodule number difficult to obtain. For all the box plots, the central rectangle extends from the first quartile to the third quartile; the line inside the rectangle represents the median; and the whiskers above and below the box indicate the positions of the maximum and minimum values, respectively.

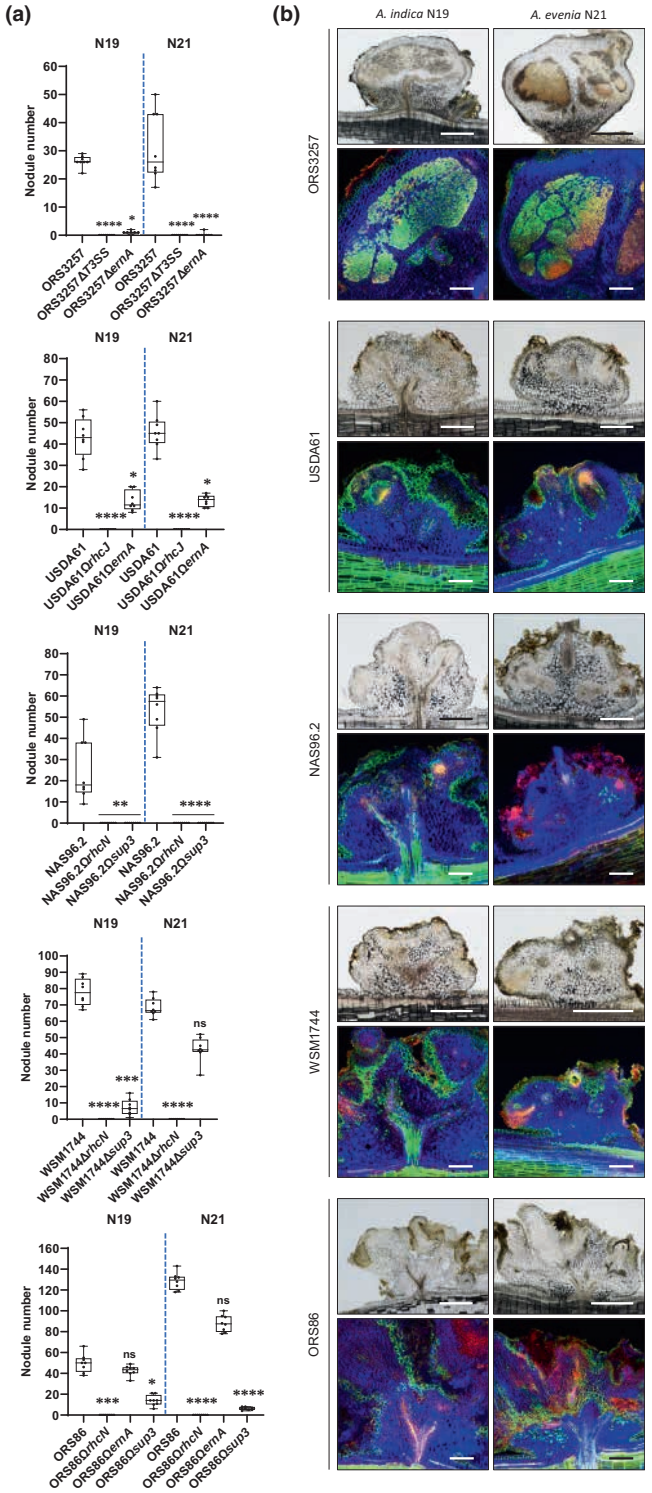

Fig. 2 Symbiotic properties of various *Bradyrhizobium* strains and their respective mutants are conserved on *Aeschynomene indica* N19 and *Aeschynomene evenia* N21. (a) Nodule number on *A. indica* N19 and *A. evenia* N21 plants at 21 d postinoculation (dpi) with five *Bradyrhizobium* strains used in this study and their respective mutants. Box plots show the results of one of the two experiments performed independently (eight plants each). The central rectangle extends from the first quartile to the third quartile; the line inside the rectangle represents the median, and the whiskers above and below the box indicate the positions of the maximum and minimum values, respectively. *, $P < 0.05$; **, $P < 0.005$; ***, $P < 0.0001$; ****, $P < 0.0001$, significant differences between the wild-type (WT) strain and each mutant using a nonparametric Kruskal–Wallis test, ns, not significant. All the mutants tested were previously obtained (Okazaki *et al*., 2009; Teulet *et al*., 2019; Camuel *et al*., 2023). (b) Upper rows: Micro-sections of nodules observed using light microscopy. Bars, 500 μm. Lower rows: confocal microscopy images of nodule sections after staining with SYTO 9 (green, live bacteria), propidium iodide (red, infected plant nuclei and dead bacteria or bacteria with compromised membranes) and calcofluor (blue, plant cell wall). Bars, 200 μm.

well as on *A. indica* N19. The 13 strains were selected based on their phylogenetic position, their predictive ET-Nod content and their ability to nodulate *A. indica* N19 (Camuel *et al*., 2023) (Fig. 1b). As shown in Fig. 1(c), for the majority of the strains belonging to the *Bradyrhizobium japonicum* or *Bradyrhizobium elkanii* phylogenetic supergroups, nodulation of *A. evenia* N76 was null or extremely reduced. Only the ORS86 strain and the three strains of the phylogenetic *Bradyrhizobium jicamae* supergroup showed a significant level of nodulation (> 20 nodules per plant). Furthermore, these 'nodules' remained often very small and their number was difficult to determine with the naked eye (Fig. S1). By contrast, on *A. evenia* N21, for the 13 strains tested, the number of nodules formed and their appearance was generally comparable to what observed on *A. indica* N19 (Figs 1c, 2).

T3SS-effectors such as ErnA and Sup3 efficiently trigger nodulation in *A. evenia* N21

To confirm that the nodulation observed on *A. evenia* N21 was T3SS-dependent and governed by the same ET-Nods as identified for *A. indica* N19, we analysed the symbiotic properties of various available mutant strains. As shown in Fig. 2, mutation of the T3SS (Ω*rhcN* or Ω*rhcJ* mutants) in five strains (ORS3257, USDA61, NAS96.2, WSM1744 and ORS86) completely aborted the nodulation on *A. evenia* N21. Furthermore, strains with mutation in different ET-Nods have the same phenotype on *A. indica* N19 and *A. evenia* N21, except for the WSM1744 strain for which the *sup3* mutation has a less drastic effect on *A. evenia* N21 (Fig. 2a). Of note, for the five strains of which mutants are tested, the pattern of nodule infection (intercellular, intracellular or not infected) on *A. indica* N19 and *A. evenia* N21 is comparable (Fig. 2b).

For the development of certain functional approaches, such as ChIP-Seq, immunoprecipitation or Turbo-ID proximity labelling to identify the nucleic or protein interactants of an ET-Nod, it may be interesting to use transgenic plants expressing only the studied ET-Nod in the absence of the bacteria and thus other potentially interfering T3Es. We have previously shown that the ectopic expression of *ernA* in *A. indica* N19 roots activates organogenesis of root- and nodule-like structures (Teulet *et al*., 2019). A similar response was observed here in transgenic hairy root lines of *A. evenia* N21 expressing *ernA* from ORS3257

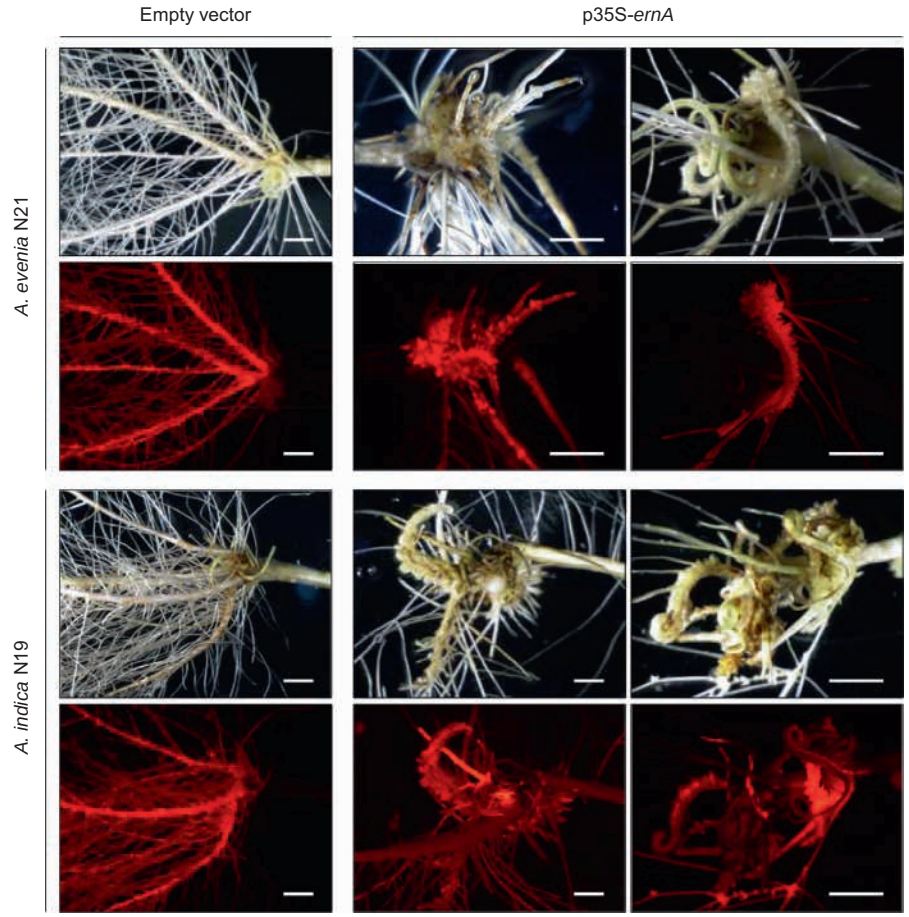

Fig. 3 Ectopic expression of *ernA* from ORS3257 in *Aeschynomene evenia* N21 and *Aeschynomene indica* N19 hairy roots. Photographs of *A. evenia* and *A. indica* roots transformed either with the empty vector containing the DsRed marker or with p35S-*ernA* at 6 wk after transformation and in the absence of bradyrhizobia. Roots were observed by a fluorescence stereomicroscope equipped with a DsRed filter. Bars, 0.3 cm. In both cases, ErnA induces nodule-like structures as previously shown in *A. indica* (Teulet *et al*., 2019).

(Fig. 3). To put the boot in, the ectopic expression of the ET-Nod *sup3* from NAS96.2 strain was also previously shown to led also to the induction of pseudo-nodules on both *A. indica* N19 and *A. evenia* N21 (Camuel *et al*., 2023). Taken together these data indicate that *A. evenia* N21/PI 225551 is an appropriate ecotype to analyse the symbiotic properties of a large diversity of *Bradyrhizobium* strains using a NF-independent, T3SS-dependent process and it can completely substitute *A. indica* N19, notably for the development of functional and transcriptomic approaches.

RNA-seq analysis reveals potential targets of ErnA in *A. evenia* N21

To better understand how ErnA activates nodule organogenesis, we compared the transcriptome of *A. evenia* N21 roots at different time points after inoculation with the WT-ORS3257 strain and the ORS3257Δ*ernA* mutant. We focused this analysis on early stages of symbiosis (2, 3, 4 and 9 dpi). It is important to note that the NF-independent, T3SS-dependent nodulation in *A. evenia* is a much slower process than the T3SS-independent process observed with photosynthetic *Bradyrhizobium* such as ORS278 or ORS285 strains. Indeed, while nodules are visible from 3 dpi with the ORS285 strain and are perfectly functional as early as 5 dpi (Bonaldi *et al*., 2011), nodules only begin to be visible from 9 dpi with ORS3257 strain and no particular plant responses are visible by the naked eye at earlier time points (Fig. 4a).

DEGs between roots inoculated with the WT and ORS3257Δ*ernA* mutant at each time point were identified with an FDR of 0.05 and a $|\text{Log}_2\text{FC}| \geq 1$ (Fig. 4c,d; Dataset S1). While at 2, 3 and 4 dpi, there were about two times more downregulated genes than upregulated genes in the WT conditions as compared with the ORS3257Δ*ern*A mutant conditions, this tendency is completely reversed at 9 dpi (Fig. 4c). This suggests that in the very early stages, one of ErnA's main functions is to repress a number of biological processes. At 9 dpi, the new wave of upregulated genes observed in WT-inoculated roots is certainly linked to the fact that nodulation and infection begin to be initiated at this point by the WT strain (Fig. 4a,b).

At 2, 3 and 4 dpi, among the categories of genes found to be the most differentially expressed (up or down) were transcription factors (TFs) with a high proportion of WRKY-TFs (eight genes) and ethylene-responsive factors (11 genes) (Fig. 4d; Dataset S1). These two families of TFs are known to be involved in plant immunity responses against pathogens attack (Tsuda & Somssich, 2015). In relation, the ACC synthase gene (Ae06g32820) which permits the synthesis of ethylene, the plant hormone defence, is one of the genes found the most strongly repressed in the WT conditions. We also observed a downregulation in

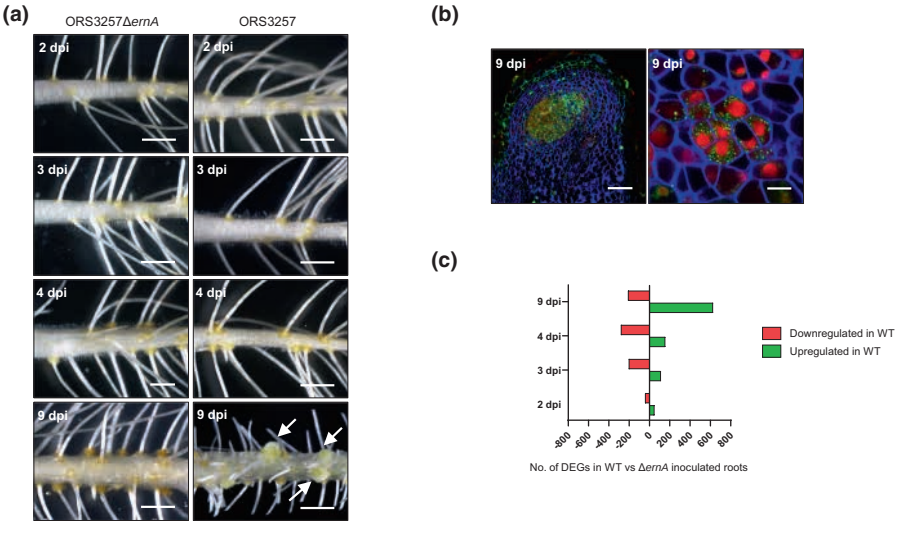

(d)

	Categories	Gene ID	DEGs 2 dpi	3 dpi	4 dpi	9 dpi
Transcription factors	WRKY-TFs	Ae07g13440*	6.4	–	-4.43	–
		Ae10g12720*	1.43	–	–	1.46
		Ae01g30690	1.25	–	–	–
		Ae07g02180	-1	-1.1	-1.18	–
		Ae10g12700	–	–	1.22	2.22
		Ae08g05500	–	–	-1.25	–
		Ae08g04850	–	–	1.2	–
		Ae02g01930	–	–	-1.08	–
	Ethylene–responsive factors	Ae06g00820	2.25	2.21	1.73	2.29
		Ae09g17160	1.89	–	–	–
		Ae04g11400	1.27	–	1.28	–
		Ae06g00840	1.22	1.71	–	–
		Ae01g03740	–	1.28	–	–
		Ae06g29920	–	-2.34	-4.62	–
		Ae09g22590	–	-1.23	–	–
		Ae02g18900	–	-1.17	-1.92	–
		Ae07g18050	–	-1.08	-1.35	-1.05
		Ae04g37530	–	–	1.36	–
		Ae06g06120	–	–	-1.17	–
	Lateral root development	Ae08g03290	–	1.06	1.04	–
		Ae03g28880	–	1.81	1.17	–
	Others	Ae06g14010	1.79	1.41	–	1.28
		Ae08g04550	1.78	–	–	–
		Ae08g04260	1.22	–	–	–
		Ae06g29380	1.07	1.49	2.04	–
		Ae05g31640	-1.88	-2.74	-3.55	-1.01
		Ae10g11050	-1.84	–	–	–
		Ae08g02860	-1.28	-1.00	–	–
		Ae04g28630	1.24	–	–	–
		Ae04g26590*	–	5.07	–	1.87
		Ae09g28280*	–	4.96	5.5	3.1
		Ae03g14060	–	1.87	–	–
		Ae04g05640	–	1.74	–	1.40
		Ae01g02360	–	1.53	–	–
		Ae09g20520	–	1.48	1.01	–
		Ae02g03760	–	1.06	1.14	–
		Ae06g00890	–	-1.89	–	–
		Ae05g12640	–	-1.71	-2.13	–
		Ae07g14510	–	-1.68	–	–
		Ae03g18120	–	-1.43	–	–
		Ae08g11470	–	-1.25	–	–
		Ae06g01880	–	-1.23	–	–
		Ae04g12060	–	-1.18	-2.23	–
		Ae01g26370	–	-1.04	-1.01	–
		Ae01g18060	–	–	3.17	1.75
		Ae04g31250	–	–	1.95	1.02
		Ae02g22290	–	–	1.34	–
		Ae10g20290	–	–	-2.47	–
		Ae01g22710	–	–	-1.67	–
		Ae04g26600	–	–	-1.13	–
		Ae09g26250	–	–	1.1	–
Plant immunity	ACC-synthase	Ae06g32820*	–	-10.73	-7.65	–
	Peroxidases	Ae05g27780	-1.05	–	–	–
		Ae01g13530	–	–	-1.60	–
	TIR-NBS-LRR	Ae07g02640	–	–	-2.97	1.34
		Ae09g03250	–	–	-1.35	–
		Ae07g02630	–	–	-1.11	–
		Ae02g04130	–	–	-1.09	–
		Ae05g30930	–	–	-1.03	–
	Other R proteins	Ae01g29070	–	-1.72	–	–
		Ae04g36510	–	-1.63	–	–
		Ae01g00100	–	-1.02	–	–
Auxin-related genes	Putative auxin transporters	Ae01g25230*	-1.36	-1.19	-1.77	–
		Ae07g18020	–	1.86	–	–
		Ae01g20380	–	1.33	–	–
		Ae04g13450	–	1.09	–	–
		Ae07g17980	–	-1.32	-1.00	–
		Ae03g22270	–	-1.28	–	–
		Ae07g18030	–	-1.05	–	–
	SAUR genes	Ae04g28180	–	–	–	2.22
		Ae04g34280	–	–	–	1.43
		Ae04g28160	–	–	–	1.19
		Ae04g34260	–	–	–	1.14
		Ae04g25150	–	–	1.97	–
		Ae06g04130	–	–	-1.55	-1.17
		Ae09g07430	–	–	–	-1.12
		Ae04g34370	–	–	–	-1.05

	Categories	Gene ID	DEGs 2 dpi	3 dpi	4 dpi	9 dpi
Signaling pathways	Receptor-like kinase	Ae01g03750	–	–	-1.54	–
		Ae09g24380	–	–	-1.46	–
		Ae08g25950	-1.66	–	–	–
		Ae05g08460	–	-2.85	–	–
		Ae02g20100*	–	-2.37	-3.67	–
		Ae06g36630	–	-2.17	–	–
		Ae08g08160	–	-1.07	-1.30	–
		Ae09g10730	–	–	4.09	–
		Ae05g01000	–	–	1.23	–
		Ae09g24400	–	–	-1.40	–
		Ae09g24230	–	–	-1.09	–
		Ae01g00180	–	-1.03	–	–
		Ae09g22250	–	–	-1.43	1.01
		Ae08g08170	–	–	-1.31	–
		Ae09g25910	–	–	-1.07	–
		Ae04g06850	–	–	-1.04	–
		Ae05g26950	–	–	-1.03	–
		Ae06g36600	–	–	-1.02	–
		Ae01g23380	–	–	-1.02	–
		Ae03g02350	–	–	-1.40	–
	Protein kinase	Ae03g24610	–	-9.09	–	-6.72
		Ae0012210	–	-7.17	–	-4.91
		Ae09g05630	–	-2.74	-3.12	–
		Ae04g02860	–	-1.50	-2.93	–
		Ae06g30620	–	-1.07	–	–
		Ae09g25900	–	–	-2.13	–
		Ae04g12170	–	-2.67	–	–
		Ae07g06130	–	-2.37	-2.38	–
		Ae04g28970	–	-2.12	-2.70	1.79
		Ae02g20010	–	–	-1.43	–
		Ae05g34560	–	–	-1.20	–
		Ae09g25850	–	–	-1.13	–
		Ae09g17300	–	1.02	–	–
Symbiotic genes	AeLB1	Ae04g33090*	–	–	–	4.14
	AeLB2	Ae04g33100	–	–	–	2.70
	AeNCR46	Ae06g25462	–	–	–	4.07
	AeNCR12	Ae02g17611	–	–	–	-2.02
	SYMREM1	Ae03g30480*	–	–	–	3.14
	AeERN1	Ae06g15750	–	–	–	-1.07
	AeERN3	Ae03g25920	–	–	–	-1.34
	PUB1	Ae03g09100	–	–	–	-1.34
Others	Cell-wall modelling	Ae06g11170	–	–	1.67	3.52
		Ae08g26160	–	–	–	2.36
		Ae04g35860	–	-3.14	–	2.17
		Ae01g25730	–	–	–	1.70
		Ae10g08500	–	–	–	1.14

Fig. 4 RNA-seq analysis between *Aeschynomene evenia* N21 roots inoculated with ORS3257 wild-type (WT) strain and its Δ*ernA* mutant. (a) Symbiotic phenotype of root plants at 2, 3, 4 and 9 d postinoculation (dpi) inoculated with ORS3257 and ORS3257Δ*ernA* mutant. Some nodules (indicated by white arrows) are visible on plant inoculated with WT strain at 9 dpi while no nodules are observed on plants inoculated with the ORS3257Δ*ernA* mutant. Bars, 500 μm. (b) Images of micro-section of nodules elicited by the WT strain showing that nodules at 9 dpi were infected intracellularly. The observations were done using a confocal microscopy after staining with SYTO 9, propidium iodide and calcofluor. Bars: (left) 200 μm; (right) 10 μm. (c) Number of differentially expressed genes (DEG) in roots inoculated with the WT strain vs ORS3257Δ*ernA* mutant at 2, 3, 4 and 9 dpi. The DEGs were defined with a false discovery rate (FDR) of 0.05 and an absolute Log_2-transformed fold change $|Log_2FC| \geq 1$. (d) Summary of the main categories of DEGs identified. A range colour from red to green indicates downregulated to upregulated genes in WT-inoculated roots vs ORS3257Δ*ernA*-inoculated roots. (*) indicate DEGs selected for real-time quantitative polymerase chain reaction analysis (RT-qPCR) and (–) indicate absence of a significant $|log_2FC|$.

WT roots of peroxidase encoding genes (Ae05g27780 and Ae01g13530) that can be involved in reactive oxygen species (ROS) production leading to oxidative burst and cell death (Almagro *et al.*, 2009). ErnA is therefore possibly involved in the repression of plant defence genes via the modulation of dedicated TFs in plant immunity control. It is also important to note the considerable number of disease resistance proteins (R proteins) that appear downregulated at 3 and 4 dpi in WT-inoculated roots. Among them, five TIR-NBS-LRR proteins have been identified. This class of R proteins are known to be involved in T3Es recognition and subsequent activation of effector-triggering immunity (ETI) (Cui *et al.*, 2015). In this sense, ErnA might prevent the recognition of other effectors injected in the host cell and avoid ETI.

The hormone auxin appears also be a key player during this interaction since the expression of several putative auxin transporters genes (eight genes) were found strongly modulated (some positively, others negatively) in the WT in comparison to the ORS3257Δ*ernA* mutant conditions (Fig. 4d). Auxin influences nearly all aspects of plant growth and development including nodule organogenesis. The importance of auxin in nodulation has been well illustrated by the application of some auxin transporter inhibitors shown to induce early nodulins and nodule organogenesis (Hirsch *et al.*, 1989; Rightmyer & Long, 2011). It is therefore possible that ErnA acts on auxin content in roots through the modulation of expression of various auxin transporters. Noteworthy is also the upregulation of several small auxin-upregulated RNA (SAUR) genes (eight genes) at 4 and 9 dpi in the WT conditions when nodulation is initiated. The SAUR genes constitute a family of auxin-responsive genes whose corresponding proteins are considered as key effector outputs of auxin signal to regulate plant growth and development (Ren & Gray, 2015). Some of the identified SAUR genes could therefore be directly involved in triggering nodulation.

Among the other remarkable DEGs identified were genes involved in signalling pathways, including several putative receptor-like kinases (20 genes) and protein kinases (13 genes). These genes have no homologue in other plants with a known function, so it is not possible to predict whether they are involved in a pathway linked to nodulation. In plants, protein kinases and receptors are often involved in pathways that detect biotic and abiotic stresses (Zhu *et al.*, 2023). Given that most of these genes were downregulated at 3 and 4 dpi in WT roots, we can speculate that this could contribute to attenuating the activation of the plant's immune system and thus indirectly facilitate symbiotic interaction. ErnA could be directly involved in the control of some of these receptor kinases.

The recent *A. evenia* genome sequencing has permitted to identify the orthologs of most known symbiotic genes characterized in the model legumes (*Medicago* and *Lotus*) (Quilbé *et al.*, 2021). We took benefit of this list of possible symbiotic genes to examine in more detail their expression during this analysis. Only a few DEG emerged and most of them were found at 9 dpi when nodules started to develop (Fig. 4d). Among the upregulated genes were found: (1) two leghemoglobin encoding genes (*AeLB1* and *AeLB2*), leghemoglobins are required to protect the nitrogenase complex from oxygen (Becana *et al.*, 2020). It is worth noting that *AeLB1* was the gene found the most upregulated at 9 dpi in the WT roots, (2) a gene encoding a Nodule cysteine-rich peptide (*AeNCR46*), NCRs are involved in the differentiation process of bacteria into bacteroids, the active nitrogen-fixing form (Czernic *et al.*, 2015); and (3) the remorin SYMREM1, shown to regulate the intracellular infection process of rhizobia (Lefebvre *et al.*, 2010). Most probably also related to this infection step observed at 9 dpi, it is noted the upregulation of several genes involved in cell wall loosening (including a polygalacturonase, *Ae08g26160*; two glucan endo-beta-glucosidases, *Ae04g35860* and *Ae10g08500*; a xyloglucan glucosylase, *Ae01g25730*; and a pectinesterase/pectinesterase inhibitor *Ae06g11170*), that most probably are required to facilitate the bacterial internalization (Fig. 4d).

A few other symbiotic genes but downregulated this time in WT-inoculated roots were also identified: (1) an NCR gene (*AeNCR12*); (2) the two Ethylene transcriptional factors ERN1 and ERN3, described to play antagonist role in the expression control of NF-elicited genes (Cerri *et al.*, 2012); and (3) the E3 ubiquitin ligase-PUB1 that negatively regulates rhizobial and mycorrhizal symbioses in *Medicago truncatula* (Vernié *et al.*, 2016).

Above transcriptomic data provide a general overview of the functions that could be modulated by ErnA and provide a first set of candidate genes whose expression could be directly targeted by it, some of which have been verified by real-time quantitative polymerase chain reaction (RT-qPCR) analysis (Fig. S2).

Mutant-based analysis of the T3SS-dependent pathways in *A. evenia* N76

Although *A. evenia* N76 is less efficiently nodulated by nonphotosynthetic bradyrhizobia using their T3SS than the accession N21, the availability of EMS mutant lines in various symbiotic genes that are required for the NF/T3SS-independent process makes this accession yet valuable to investigate whether these determinants are also recruited during the T3SS-dependent nodulation process.

We analysed the symbiotic properties of five nonphotosynthetic *Bradyrhizobium* strains, for which nodulation to varying degrees was previously observed on *A. evenia* WT N76, on six mutant lines (*crk*, *pollux*, *ccamk*, *cyclops*, *nsp2* and *nin*) (Fig. 1c). It should be noted that no nodules are observed on these six mutant lines when they are inoculated with photosynthetic bradyrhizobia such as ORS278 strain (Fig. 5a), (Quilbé *et al.*, 2021). For the five analysed strains, a number of common observations could be done (Fig. 5a): (1) no significant difference in the number of nodules was observed between the WT and the *crk* mutant and (2) no nodulation was observed for the *nsp2* and *nin* mutants. These data are informative as they indicate on the one hand that CRK is dispensable for the T3SS-dependent symbiotic process and, on the other hand, that this signalling pathway requires NIN and NSP2 like the other symbiotic nitrogen-fixing processes described to date.

The impact of the mutations in the symbiotic determinants POLLUX, CCaMK and CYCLOPS depended on the strain tested: (1) for the two strains (ORS3257 and LMG09283), no nodules were observed on these three mutant lines; (2) for the two strains (CCBAU23086 and WSM1744), the *pollux* and *ccamk* mutations completely aborted nodulation, while a few nodules could still be observed in the *cyclops* mutant for CCBAU23086, and this mutation has no effect on nodulation for WSM1744 (Fig. 5a); and finally (3) for the ORS86 strain, nodules could be observed in all three mutant lines (Fig. 5a,b). These results indicate that several symbiotic determinants are dispensable in *A. evenia* for nodulation by certain *Bradyrhizobium* strains using their T3SS.

Cooperativity between ET-Nods for nodulation activation

These observed differences between the strains may be explained by the fact that each of them injects a specific set of T3Es. In particular, the ORS86 strain, which can bypass the mutation of several canonical symbiotic genes, has two ET-Nods (ErnA and Sup3). We examined in this strain the effect of the mutation of each ET-Nod as well as the effect of the T3SS mutation. As expected, inactivation of the T3SS completely abolished nodulation, confirming that the nodules induced on WT *A. evenia* N76 plants are dependent on T3SS (Fig. 5c). Inactivation of *ernA* or *sup3* significantly reduced the number of nodules on WT N76 plants suggesting that these two ET-Nods act synergistically to activate nodulation. This synergistic effect seems to be essential to bypass the mutation of plants in *POLLUX, CCaMK, CYCLOPS*. Indeed, the Ω*sup3* mutant strain was unable to induce nodules in these three *A. evenia* mutant lines, while the Ω*ernA* mutant strain only induced a few nodules in the *pollux* mutant (Fig. 5c).

As Sup3 is the only difference in the ET-Nod content between the ORS86 and ORS3257 strains, we also investigated the effect of introducing this T3E into ORS3257 and its ORS3257Δ*ernA* mutant. Since previous functional data were obtained with the Sup3 of WSM1744 strain (Camuel *et al.*, 2023), we decided to work with this homologue. The data obtained confirm the synergistic effect between these two ET-Nods, as the addition of $sup3_{WSM1744}$ in the WT strain ORS3257 resulted in a 4 times higher nodulation capacity on the WT N76 and the *crk* mutant plants (Figs 5d, S3). However, this synergistic effect appears to be more limited than that observed with the ORS86 strain, since no nodules were formed on the other plant mutant lines tested, with the exception of the *cyclops* mutant, where a nodule was occasionally observed on some plants (two plants out of eight with one nodule). Given that ORS3257 induced a very low number of nodules on WT N76 plants compared with ORS86, this difference observed with strain ORS86 could be due to incompatibility factors (T3Es, or surface polysaccharide compounds), which could compromise the symbiosis. In the ORS3257Δ*ernA* mutant, the addition of $sup3_{WSM1744}$ restored nodulation to a level comparable to that of the ORS3257 WT strain, but did not facilitate nodulation in the *cyclops* mutant (Figs 5d, S3).

Taken together, these data indicate that ET-Nods can have a cumulative effect on the activation of nodule organogenesis and allow some strains to nodulate plants with mutations in key symbiotic determinants such as POLLUX, CCaMK and CYCLOPS.

Discussion

The model legume *A. evenia* for the study of the T3SS-dependent symbiotic process

The discovery of a novel alternative symbiotic pathway between bradyrhizobia and legumes based on the T3SS is recent (Okazaki *et al.*, 2013). If progresses have been made these last years on the bacterial partner through the identification of various T3Es triggering nodulation in the absence of NFs, nothing is known on their mode of action and on the plant pathways activated after their translocation into the host cell.

So far, only certain species of two legume genera have been shown to have the capacity to be nodulated via a T3SS-dependent process: (1) the *Glycine max* (soybean) cultivar Enrei which can be nodulated by a *nodC* mutant of *B. elkanii* USDA61 (Okazaki *et al.*, 2013); and (2) several *Aeschynomene* species including *A. indica* which has been preferentially used given its robust nodulation response to a large diversity of *Bradyrhizobium* strains (Okazaki *et al.*, 2016).

Like most legumes, *Glycine max* uses in nature a NF-dependent process. Thus, to decipher the molecular mechanism specific to the T3SS process in this legume species, the use of a plant mutant in the NF receptors (like *nfr1* (Ikeda *et al.*, 2008)), and/or a bacterial mutant affected in the *nod* genes is necessary (Okazaki *et al.*, 2013). By contrast, in the NF-independent *Aeschynomene* species, an interference with NF-mediated activation is less likely to occur, although genes encoding NF receptors (NFP/LYK3) are present in *A. evenia*, several indications suggest that these genes are not functional (Quilbé *et al.*, 2021). Furthermore, *nod* gene mutants of strains USDA61 and ORS285 nodulate *A. indica* as well as the original WT strains showing that NFs are not necessary to activate nodulation in such species (Bonaldi *et al.*, 2011; Okazaki *et al.*, 2016). This is consistent with the fact that NF-independent *Aeschynomene* spp. are naturally nodulated by photosynthetic bradyrhizobia lacking *nod* genes (Giraud *et al.*, 2007).

Among the NF-independent *Aeschynomene* species, *A. evenia* N76 was chosen as model plant to decipher at the plant level the molecular mechanism of the NF-independent, T3SS-independent symbiotic process used by photosynthetic bradyrhizobia (Arrighi *et al.*, 2012). The T3SS-dependent interaction is much specific because the reference *A. evenia* line N76 is poorly nodulated by the majority of nonphotosynthetic *Bradyrhizobium* strains. This bradyrhizobial selectivity is shared by most of the accessions tested here except for three accessions, including N21, which belongs to the same ecotype. Strikingly, *A. evenia* N21 showed a high nodulation efficiency and was permissive to a large set of *Bradyrhizobium* strains using their T3SS as evidenced previously for *A. indica* (Okazaki *et al.*, 2016). The contrasting responses of the N21 and N76 to nonphotosynthetic bradyrhizobia provide an opportunity to search for the genetic determinant(s) that control(s) rhizobium promiscuity, a nodulation trait that is still poorly understood in legumes. In addition, the selected N21 line can be used in pair with the reference line N76 to investigate now different NF-independent nodulation processes in the *Bradyrhizobium-A. evenia* symbiotic system.

RNA-seq analysis reveals a dual role of ErnA in plant defence responses and nodule organogenesis

The usefulness of the *A. evenia* N21 accession to progress in the understanding of the T3SS-dependent process was demonstrated in this study by investigating the genes modulated by ErnA. By comparing the transcriptome of *A. evenia* N21 roots inoculated with the ORS3257 WT or its derivative Δ*ernA* mutant, two main

functional groups emerged: the repression in the roots inoculated by the WT strain of numerous plant defence genes and the modulation, positively or negatively, of several genes related in auxin transport and signalling, a key hormone involved in root and nodule development (Mathesius, 2008). Interestingly, a similar transcriptomic analysis was recently performed in *Glycine max nfr1* roots inoculated with USDA61 WT strain and its derivative *bel2-5* mutant, Bel2-5 was shown to be the key T3Es governing nodulation during this latter interaction (Ratu *et al.*, 2021). This study also revealed the repression of plant defence genes in WT-inoculated *Glycine max* roots. While auxin-related genes were not shown to be differentially expressed, several genes involved in cytokinin biosynthesis are upregulated in the WT conditions. As the hormone cytokinin also plays a key role in nodule organogenesis (Boivin *et al.*, 2016), we hypothesize that the ET-Nods ErnA and Bel2-5 play a similar dual role. On the one hand, they repress the plant immune system to allow intracellular acceptance of bacteria, and on the other hand, they activate nodule organogenesis

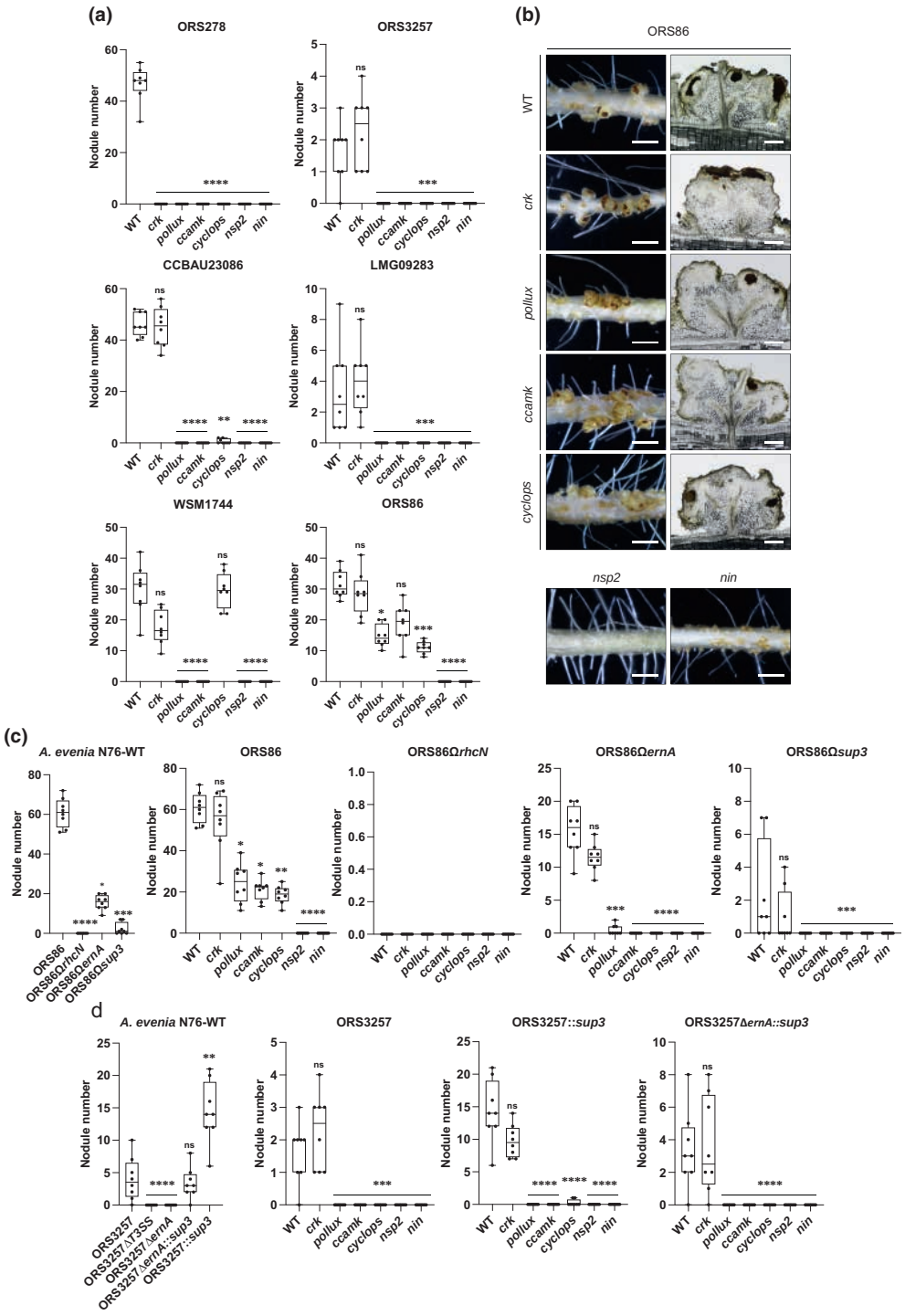

Fig. 5 Some *Bradyrhizobium* strains can nodulate certain *Aeschynomene evenia* N76 mutant lines affected in key symbiotic genes and this required a synergetic role of effectors triggering nodulation (ET-Nods) during type III secretion system (T3SS)-dependent symbiosis. (a) Nodule number on wild-type (WT) *A. evenia* N76 and its different ethyl methane sulfonate (EMS) mutant lines (*crk*, *pollux*, *ccamk*, *cyclops*, *nsp2* and *nin*) after inoculation with the photosynthetic *Bradyrhizobium* ORS278 strain using a T3SS-independent process and five others *Bradyrhizobium* strains (ORS3257, LMG09283, CCBAU23086, WSM1744 and ORS86) able to nodulate *A. evenia* N76 using their T3SS. Observations were made at 21 d postinoculation (dpi). Box plots show the results of one of the two experiments performed independently (eight plants each). *, $P \leq 0.01$; **, $P \leq 0.001$; ***, $P \leq 0.0005$; ****, $P < 0.0001$, significant differences between the WT line and each EMS mutant lines using a nonparametric Kruskal–Wallis test, ns, not significant. (b) Column 1: photograph of roots and nodules induced by ORS86 on *A. evenia* N76 plants and its EMS mutant lines. Column 2: Micro-sections of nodules observed using light microscopy. Bars: (row 1) 0.2 cm; (row 2) 250 μm. (c) Nodule number on WT *A. evenia* N76 and its different EMS mutant lines (*crk*, *pollux*, *ccamk*, *cyclops*, *nsp2* and, *nin*) after inoculation with ORS86 and its respective mutants in T3SS (Ω*rhcN*) and the two identified ET-Nods (Ω*ernA* and Ω*sup3*). Box plots show the results of one of the two experiments performed independently (eight plants each). *, $P < 0.05$; ***, $P < 0.001$; ****, $P < 0.0001$, significant differences between the WT and the mutants (plant or bacteria) using a nonparametric Kruskal–Wallis test, ns, not significant. (d) Effect of the addition of the $sup3_{WSM1744}$ gene into ORS3257 and its ORS3257Δ*ernA* mutant on the nodulation of WT *A. evenia* N76 and its EMS mutant lines. **, $P < 0.01$; ***, $P < 0.001$; ****, $P < 0.0001$, significant differences between the WT strain (or the WT plant) and each mutant using a nonparametric Kruskal–Wallis test, ns, not significant. All box plots show the results of one of the two experiments performed independently (eight plants each). For all the box plots, the central rectangle extends from the first quartile to the third quartile; the line inside the rectangle represents the median, and the whiskers above and below the box indicate the positions of the maximum and minimum values, respectively.

by modulating the cytokine/auxin balance but using different pathways.

This RNA-seq analysis revealed a long list of candidate genes that could be direct targets of ErnA, including genes encoding transcription factors, genes involved in plant signalling or genes related to plant hormone synthesis or signalling. One of the precautions to be taken in this type of experiment is that the bacterium injects a cocktail of effectors into the host cell and that these effectors may interact antagonistically or synergistically (Teulet *et al.*, 2022). Although an isogenic Δ*ernA* mutant is used, it cannot be excluded that the observed effects are the consequence of other effectors that arise due to the absence of ErnA. To overcome this type of 'artefact' and to narrow the list of possible ErnA targets, experiments are in progress to conduct transcriptomic analyses of *A. evenia* roots overexpressing *ernA* using a dexamethasone-inducible promoter (pDEX). The fact that roots of the *A. evenia* N21 line overexpressing *ernA*, like *A. indica* roots, form nodule-like structures is encouraging to pursue this type of approach.

It may be puzzling that some symbiotic genes (POLLUX, CCaMK, CYCLOPS, NSP2 and NIN) that have been shown to be required during the ORS3257/*A. evenia* symbiosis (to be described later) were not found to be differentially expressed between roots inoculated with the WT strain and the ORS3257Δ*ernA* mutant. In fact, several of these genes (POLLUX, CCaMK and NSP2), which are initially expressed in non-inoculated roots, are also not found to be overexpressed during nodulation in other symbiotic models (*Medicago*, *Lotus* and *Aeschynomene* nodulated, respectively, by *S. meliloti*, *M. loti* and *Bradyrhizobium* sp. ORS278) (Benedito *et al.*, 2008; Mun *et al.*, 2016; Gully *et al.*, 2018; Quilbé *et al.*, 2022). Only NIN and CYCLOPS expression was found to be upregulated during nodulation in these different symbiotic processes. In the case of the ORS278/*A. evenia* interaction, NIN overexpression was only detected from the time point (4 dpi) when nodules were clearly visible and CYCLOPS only in mature nodule at 7 and 14 dpi (Gully *et al.*, 2018; Quilbé *et al.*, 2022). The absence of differential expression of NIN and CYCLOPS between roots inoculated with the ORS3257 WT strain and the ORS3257Δ*ernA* mutant could be therefore explained by the fact that the transcriptomic analysis was carried out at a stage that is still too early (the T3SS-dependent process being a much slower process), and also by the fact that the RNA-seq analysis was carried out on whole roots, which could mask a highly localized specific expression. As the bacteria specifically colonize the axillary root hairs at the base of lateral roots, a very localized expression of genes after injection of T3Es into these plant cells can be assumed. For a more detailed transcriptomic analysis, it would be interesting to use single-cell RNA sequencing technology, which is extremely powerful in detecting very local changes in expression levels and is beginning to be used to study rhizobium–legume symbiotic interactions in other model legumes (Cervantes-Pérez *et al.*, 2022; Frank *et al.*, 2023; Liu *et al.*, 2023).

Some key determinants of the NF-signalling pathway are recruited during the T3SS-dependent process

Distinct ET-Nods were identified in T3SS-containing *Bradyrhizobium* strains (Camuel *et al.*, 2023). To make a first determination of whether these various ET-Nods act at different levels of the plant signalling pathways, we took advantage of several *A. evenia* N76 mutant lines unable to form nodules with the model strain ORS278 that uses a NF/T3SS-independent process. This analysis provided several interesting insights. First, the *AeCRK* determinant encoding a CRK, which has been shown to be necessary for NF-independent nodulation by strain ORS278 (Quilbé *et al.*, 2021, 2022), is dispensable in the case of strains using a T3SS-dependent process. CRK is thought to be part of a receptor complex sensing non-Nod symbiotic signal(s) synthesized by photosynthetic bradyrhizobia that remains to be disclosed. Bradyrhizobia that use a T3SS-dependent process and inject a set of effectors directly into the host cell thus probably do not need this first initial recognition step by plant membrane receptors to activate nodulation. These observations reinforce the idea that *Ae*CRK acts in the very early stages of NF/T3SS-independent.

Second, the NSP2 and NIN transcriptional factors are key determinants of the T3SS-dependent pathway since all the five tested strains were Nod$^-$ on the corresponding mutants. These

data suggest that the different ET-Nods identified in these five strains (ErnA, Sup3, Ubi1, Ubi2 and Ubi3) all act, in combination or alone, upstream of these two TFs to activate the nodulation process.

Third, some canonical symbiotic genes are dispensable for some *Bradyrhizobium* strains to activate nodulation in a T3SS-dependent manner. For example, strain WSM1744, and strain CCBAU23086 at a lower level, can induce nodules on a *cyclops* mutant. This observation is surprising as these two strains have a Nod^- phenotype on the *ccamk* mutant, while in the NF-signalling pathway, CYCLOPS acts downstream of CCaMK. In this pathway, CYCLOPS phosphorylation by CCaMK activates the expression of related symbiotic genes including NIN (Singh *et al.*, 2014). To explain our data, we could assume that CCaMK phosphorylates other actors than CYCLOPS that also play a prominent role in the activation of nodulation. The hypothesis that CCaMK has other yet unknown targets (X) has already been proposed by Limpens & Bisseling (2014) to explain the divergent symbiotic phenotypes observed between *cyclops* and *ccamk* mutants in *Lotus japonicus*.

The symbiotic phenotype of strain ORS86 is also amazing as this strain is able to bypass the requirement of several key symbiotic genes (POLLUX, CCaMK and CYCLOPS) for nodulation. This strain has previously been shown to be one of the most efficient strains in nodule induction on *A. indica* plants and the same was found with the *A. evenia* N76 line. The ORS86 strain has two ET-Nods (ErnA and Sup3), and we showed that both of them are required to bypass the POLLUX, CCaMK and CYCLOPS mutations, suggesting that they act synergistically to trigger nodulation. At this stage, it is difficult to envisage how this cooperativity between these two ET-Nods works. Do they act at different levels of the signalling pathway or do they intervene on the same actor(s) and by cumulating their action allow them to reach a sufficient 'threshold' level to trigger the nodule organogenesis process? These important questions remain to explored in future research to better understand the T3SS-dependent process.

In conclusion, this study identified the *A. evenia* N21 accession as suitable for functional analyses to elucidate the molecular mechanisms of the T3SS-dependent nodule organogenesis. While this research can benefit of all the genetic tools and data acquired on the closely related *A. evenia* N76 that is used to study the NF/T3SS-independent nodulation process, the promiscuous nodulation character of the N21 accession makes it highly fitting to investigate the multiple mechanisms by which different ET-Nods can induce nodulation.

The identification of possible targets of ErnA by the RNA-seq analysis as well as the evidences that T3SS-dependent nodule organogenesis requires some classical symbiotic determinants such as NSP2 and NIN and that others can be dispensable constitute major advances in the understanding of this process. Identifying the targets of ET-Nods and understanding their mode of action are important knowledge gaps that need to be filled now. This knowledge will provide insights into the functioning of the root nodule symbiosis and could contribute to the development of a more sustainable agriculture. Furthermore, understanding by which mechanisms the bacterium can bypass several key players in the symbiotic/nodulation signalling pathway while continuing to induce nodule organogenesis may also be an important avenue to explore in the future to transfer the symbiotic capacity to cereals.

Acknowledgements

This work was supported by a grant from the French National Research Agency ('ET-Nod'; ANR-20-CE20-0012-01). AC was supported by a PhD fellowship from the French Ministry of National Education, Higher Education and Research.

Competing interests

None declared.

Author contributions

AC, J-FA and EG conceived and designed the study. AC, MP, DG, AT, NN and EG performed the experiments and analysed the results. AC, J-FA and EG wrote the manuscript. All authors commented on the results and the manuscript. J-FA and EG contributed equally to this work.

ORCID

Jean-François Arrighi https://orcid.org/0000-0001-6184-2066
Alicia Camuel https://orcid.org/0000-0003-3912-9613
Eric Giraud https://orcid.org/0000-0002-4190-1732
Djamel Gully https://orcid.org/0000-0003-1695-5744
Nico Nouwen https://orcid.org/0000-0002-7132-9378
Marjorie Pervent https://orcid.org/0000-0002-2429-1389
Albin Teulet https://orcid.org/0000-0002-3188-7260

Data availability

The data of the RNA-seq analysis are available at NCBI BioProject (accession: hite). The data supporting the findings of this study are available within the article and its Supporting Information (Figs S1–S3; Tables S1–S4; Dataset S1).

References

Almagro L, Gómez Ros LV, Belchi-Navarro S, Bru R, Ros Barceló A, Pedreño MA. 2009. Class III peroxidases in plant defence reactions. *Journal of Experimental Botany* **60**: 377–379.

Arrighi JF, Cartieaux F, Brown SC, Rodier-Goud M, Boursot M, Fardoux J, Patrel D, Gully G, Fabre S, Chaintreuil C *et al.* 2012. Aeschy*nomene evenia*, a model plant for studying the molecular genetics of the Nod- independent rhizobium-legume symbiosis. *Molecular Plant–Microbe Interactions* **25**: 851–861.

Becana M, Yruela I, Sarath G, Catalán P, Hargrove MS. 2020. Plant hemoglobins: a journey from unicellular green algae to vascular plants. *New Phytologist* **227**: 1618–1635.

Benedito VA, Torres-Jerez I, Murray JD, Andriankaja A, Allen S, Kakar K, Wandrey M, Verdier J, Zuber H, Ott T *et al.* 2008. A gene expression atlas of the model legume *Medicago truncatula*. *The Plant Journal* **55**: 504–513.

Boivin S, Fonouni-Farde C, Frugier F. 2016. How auxin and cytokinin phytohormones modulate root microbe interactions. *Frontiers in Plant Science* **7**: 1240.

Bonaldi K, Gargani D, Prin Y, Fardoux J, Gully D, Nouwen N, Goormachtig S, Giraud E. 2011. Nodulation of *Aeschynomene afraspera* and *A. indica* by photosynthetic *Bradyrhizobium* sp. strain ORS285: the nod-dependent versus the nod- independent symbiotic interaction. *Molecular Plant–Microbe Interactions* **24**: 1359–1371.

Bonaldi K, Gherbi H, Franche C, Bastien G, Fardoux J, Barker D, Giraud E, Cartieaux F. 2010a. The Nod factor-independent symbiotic signaling pathway: development of *Agrobacterium rhizogenes*-mediated transformation for the legume *Aeschynomene indica*. *Molecular Plant–Microbe Interactions* **23**: 1537–1544.

Bonaldi K, Gourion B, Fardoux J, Hannibal L, Cartieaux F, Boursot M, Vallenet D, Chaintreuil C, Prin Y, Nouwen N *et al.* 2010b. Large-scale transposon mutagenesis of photosynthetic *Bradyrhizobium* sp. strain ORS278 reveals new genetic loci putatively important for Nod-independent symbiosis with *Aeschynomene indica*. *Molecular Plant–Microbe Interactions* **23**: 760–770.

Busset N, Gully D, Teulet A, Fardoux J, Camuel A, Cornu D, Severac D, Giraud E, Mergaert P. 2021. The Type III effectome of the symbiotic *Bradyrhizobium vignae* strain ORS3257. *Biomolecules* **11**: 1592.

Camuel A, Teulet A, Carcagno M, Haq F, Pacquit V, Gully D, Pervent M, Chaintreuil C, Fardoux J, Horta-Araujo N *et al.* 2023. Widespread *Bradyrhizobium* distribution of diverse Type III effectors that trigger legume nodulation in the absence of Nod factor. *The ISME Journal* **17**: 1416–1429.

Cassan O, Lèbre S, Martin A. 2021. Inferring and analyzing gene regulatory networks from multi-factorial expression data: a complete and interactive suite. *BMC Genomics* **22**: 387.

Cerri MR, Frances L, Laloum T, Auriac MC, Niebel A, Oldroyd GE, Barker DG, Fournier J, de Carvalho-Niebel F. 2012. *Medicago truncatula* ERN transcription factors: regulatory interplay with NSP1/NSP2 GRAS factors and expression dynamics throughout rhizobial infection. *Plant Physiology* **160**: 2155–2172.

Cervantes-Pérez SA, Thibivilliers S, Laffont C, Farmer AD, Frugier F, Libault M. 2022. Cell-specific pathways recruited for symbiotic nodulation in the *Medicago truncatula* legume. *Molecular Plant* **15**: 1868–1888.

Chaintreuil C, Perrier X, Martin G, Fardoux J, Lewis GP, Brottier L, Rivallan R, Gomez-Pacheco M, Bourges M, Lamy L *et al.* 2018. Naturally occurring variations in the nod-independent model legume *Aeschynomene evenia* and relatives: a resource for nodulation genetics. *BMC Plant Biology* **18**: 54.

Chomczynski P, Sacchi N. 1987. Single-step method of RNA isolation by acid guanidinium thiocyanate-phenol-chloroform extraction. *Analytical Biochemistry* **162**: 156–159.

Cui H, Tsuda K, Parker JE. 2015. Effector-triggered immunity: from pathogen perception to robust defense. *Annual Review of Plant Biology* **66**: 487–511.

Czernic P, Gully D, Cartieaux F, Moulin L, Guefrachi I, Patrel D, Pierre O, Fardoux J, Chaintreuil C, Nguyen P *et al.* 2015. Convergent evolution of endosymbiont differentiation in dalbergioid and inverted repeat-lacking clade legumes mediated by nodule- specific cysteine-rich peptides. *Plant Physiology* **169**: 1254–1265.

Dobin A, Davis CA, Schlesinger F, Drenkow J, Zaleski C, Jha S, Batut P, Chaisson M, Gingeras TR. 2013. STAR: ultrafast universal RNA-seq aligner. *Bioinformatics* **29**: 15–21.

Ewels PA, Peltzer A, Fillinger S, Patel H, Alneberg J, Wilm A, Garcia MU, Di Tommaso P, Nahnsen S. 2020. The nf-core framework for community-curated bioinformatics pipelines. *Nature Biotechnology* **38**: 276–278.

Feng J, Lee T, Schiessl K, Oldroyd GED. 2021. Processing of NODULE INCEPTION controls the transition to nitrogen fixation in root nodules. *Science* **374**: 629–632.

Frank M, Fechete LI, Tedeschi F, Nadzieja M, Nørgaard MMM, Montiel J, Andersen KR, Schierup MH, Reid D, Andersen SU. 2023. Single-cell analysis identifies genes facilitating rhizobium infection in *Lotus japonicus*. *Nature Communications* **14**: 7171.

Giraud E, Moulin L, Vallenet D, Barbe V, Cytryn E, Avarre JC, Jaubert M, Simon D, Cartieaux F, Prin Y *et al.* 2007. Legumes symbioses: absence of *nod* genes in photosynthetic bradyrhizobia. *Science* **316**: 1307–1312.

Gully D, Czernic P, Cruveiller S, Mahé F, Longin C, Vallenet D, François P, Nidelet S, Rialle S, Giraud E *et al.* 2018. Transcriptome profiles of Nod factor-independent symbiosis in the tropical legume *Aeschynomene evenia*. *Scientific Reports* **8**: 10934.

Hirsch AM, Bhuvaneswari TV, Torrey JG, Bisseling T. 1989. Early nodulin genes are induced in alfalfa root outgrowths elicited by auxin transport inhibitors. *Proceedings of the National Academy of Sciences, USA* **86**: 1244–1248.

Ikeda S, Rallos LEE, Okubo T, Eda S, Inaba S, Mitsui H, Minamisawa K. 2008. Microbial community analysis of field-grown soybeans with different nodulation phenotypes. *Applied and Environmental Microbiology* **74**: 5704–5709.

Lefebvre B, Timmers T, Mbengue M, Moreau S, Herve C, Toth K, Bittencourt-Silvestre J, Klaus D, Deslandes L, Godiard L *et al.* 2010. A remorin protein interacts with symbiotic receptors and regulates bacterial infection. *Proceedings of the National Academy of Sciences, USA* **107**: 2343–2348.

Letunic I, Bork P. 2021. Interactive tree of life (iTOL) v5: an online tool for phylogenetic tree display and annotation. *Nucleic Acids Research* **49**: W293–W296.

Limpens E, Bisseling T. 2014. CYCLOPS: a new vision on rhizobium-induced nodule organogenesis. *Cell Host & Microbe* **15**: 127–129.

Liu Z, Yang J, Long Y, Zhang C, Wang D, Zhang X, Dong W, Zhao L, Liu C, Zhai J *et al.* 2023. Single-nucleus transcriptomes reveal spatiotemporal symbiotic perception and early response in *Medicago*. *Nature Plants* **9**: 1734–1748.

Love MI, Huber W, Anders S. 2014. Moderated estimation of fold change and dispersion for RNA-Seq data with DESEQ2. *Genome Biology* **15**: 1–21.

Mathesius U. 2008. Auxin: at the root of nodule development? *Functional Plant Biology* **35**: 651–668.

Mun T, Bachmann A, Gupta V, Stougaard J, Andersen SU. 2016. Lotus base: an integrated information portal for the model legume *Lotus japonicus*. *Scientific Reports* **6**: 39447.

Okazaki S, Kaneko T, Sato S, Saeki K. 2013. Hijacking of leguminous nodulation signaling by the rhizobial type III secretion system. *Proceedings of the National Academy of Sciences, USA* **110**: 17131–17136.

Okazaki S, TIttabutr P, Teulet A, Thouin J, Fardoux J, Chaintreuil C, Gully D, Arrighi JF, Furuta N, Miwa H *et al.* 2016. Rhizobium–legume symbiosis in the absence of Nod factors: two possible scenarios with or without the T3SS. *The ISME Journal* **10**: 641–674.

Okazaki S, Zehner S, Hempel J, Lang K, Göttfert M. 2009. Genetic organization and functional analysis of the type III secretion system of *Bradyrhizobium elkanii*. *FEMS Microbiology Letters* **295**: 88–95.

Oldroyd GED. 2013. Speak, friend, and enter: signalling systems that promote beneficial symbiotic associations in plants. *Nature Reviews Microbiology* **11**: 252–263.

Patel H, Ewels P, Peltzer A, Hammarén R, Botvinnik O, Sturm G, Moreno D, Vemuri P, Morins S, Pantano L *et al.* 2020. nf-core/rnaseq: nf-core/rnaseq v.3.0 -Silver Shark. *Zenodo*. doi: 10.5281/zenodo.4323183.

Patro R, Duggal G, Love MI, Irizarry RA, Kingsford C. 2017. Salmon provides fast and bias-aware quantification of transcript expression. *Nature Methods* **14**: 17–419.

Perret X, Staehelin C, Broughton WJ. 2000. Molecular basis of symbiotic promiscuity. *Microbiology and Molecular Biology Reviews* **64**: 180–201.

Quilbé J, Lamy L, Brottier L, Leleux P, Fardoux J, Rivallan R, Benichou T, Guyonnet R, Becana M, Villar I *et al.* 2021. Genetics of nodulation in *Aeschynomene evenia* uncovers mechanisms of the rhizobium-legume symbiosis. *Nature Communications* **12**: 829.

Quilbé J, Nouwen N, Pervent M, Guyonnet R, Cullimore J, Gressent F, Araújo NH, Gully D, Klopp C, Giraud E *et al.* 2022. A mutant-based analysis of the establishment of Nod-independent symbiosis in the legume *Aeschynomene evenia*. *Plant Physiology* **190**: 1400–1417.

Ratu STN, Teulet A, Miwa H, Masuda S, Nguyen HP, Yasuda M, Sato S, Kaneko T, Hayashi M, Giraud E *et al.* 2021. Rhizobia use a pathogenic-like effector to hijack leguminous nodulation signaling. *Scientific Reports* **11**: 2034.

Ren H, Gray WM. 2015. SAUR proteins as effectors of hormonal and environmental signals in plant growth. *Molecular Plant* **8**: 1153–1164.

Rightmyer AP, Long SR. 2011. Pseudonodule formation by wild-type and symbiotic mutant *Medicago truncatula* in response to auxin transport inhibitors. *Molecular Plant–Microbe Interactions* **24**: 1372–1384.

Roy S, Liu W, Nandety RS, Crook A, Mysore KS, Pislariu CI, Frugoli J, Dickstein R, Udvardi MK. 2020. Celebrating 20 years of genetic discoveries in legume nodulation and symbiotic nitrogen fixation. *Plant Cell* **32**: 15–41.

Sadowsky MJ, Tully RE, Cregan PB, Keyser HH. 1987. Genetic diversity in *Bradyrhizobium japonicum* serogroup 123 and its relation to genotype-specific nodulation of soybean. *Applied and Environmental Microbiology* **53**: 2624–2630.

Sambrook J, Fritsch EF, Maniatis TA. 1989. *Molecular cloning: a laboratory manual, 2nd edn.* Cold Spring Harbor, NY, USA: Cold Spring Harbor Laboratory.

Singh S, Katzer K, Lambert J, Cerri M, Parniske M. 2014. CYCLOPS, a DNA-binding transcriptional activator, orchestrates symbiotic root nodule development. *Cell Host & Microbe* **15**: 139–152.

Songwattana P, Chaintreuil C, Wongdee J, Teulet A, Mbaye M, Piromyou P, Gully D, Fardoux J, Zoumman AMA, Camuel A *et al.* 2021. Identification of type III effectors modulating the symbiotic properties of *Bradyrhizobium vignae* strain ORS3257 with various *Vigna* species. *Scientific Reports* **11**: 4874.

Teulet A, Busset N, Fardoux J, Gully D, Chaintreuil C, Cartieaux F, Jauneau A, Comorge V, Okazaki S, Kaneko T *et al.* 2019. The rhizobial type III effector ErnA confers the ability to form nodules in legumes. *Proceedings of the National Academy of Sciences, USA* **116**: 21758–21768.

Teulet A, Camuel A, Perret X, Giraud E. 2022. The versatile roles of Type III secretion systems in rhizobium-legume symbioses. *Annual Review of Microbiology* **76**: 45–65.

Tsuda K, Somssich IE. 2015. Transcriptional networks in plant immunity. *New Phytologist* **206**: 932–947.

Vernié T, Camut S, Camps C, Rembliere C, de Carvalho-Niebel F, Mbengue M, Timmers T, Gasciolli V, Thompson R, le Signor C *et al.* 2016. PUB1 interacts with the receptor kinase DMI2 and negatively regulates rhizobial and arbuscular mycorrhizal symbioses through its ubiquitination activity in *Medicago truncatula*. *Plant Physiology* **170**: 2312–2324.

Vincent J. 1970. *A manual for the practical study of root-nodule bacteria.* Oxford, UK: Blackwell Scientific.

Zhu Q, Feng Y, Xue J, Chen P, Zhang A, Yu Y. 2023. Advances in receptor-like protein kinases in balancing plant growth and stress responses. *Plants* **12**: 427.

Supporting Information

Additional Supporting Information may be found online in the Supporting Information section at the end of the article.

Dataset S1 List of differentially expressed genes.

Fig. S1 Symbiotic phenotype of 13 selected *Bradyrhizobium* strains on *Aeschynomene* spp. (*A. indica* N19 and *A. evenia* N76/N21).

Fig. S2 RT-qPCR of some genes emerging in the RNA-seq analysis in *Aeschynomene evenia* inoculated with the ORS3257 wild-type strain or with its Δ*ernA* mutant.

Fig. S3 Synergetic role of ET-Nods during T3SS-dependent symbiosis.

Table S1 Plant accessions used in this study, origin and characteristics.

Table S2 Strains and mutants used in this study, origin and characteristics.

Table S3 Summary of raw Illumina sequencing and filtered reads after trimming and alignment of reads to *Aeschynomene evenia* v1 genome in each library.

Table S4 List of primers used for RT-qPCR.

Please note: Wiley is not responsible for the content or functionality of any Supporting Information supplied by the authors. Any queries (other than missing material) should be directed to the *New Phytologist* Central Office.